ADVANCED MULTIFIELD MODELS FOR WAVES PROPAGATION ANALYSIS IN METALLIC PANELS

Jamal Najd, Enrico Zappino, Erasmo Carrera, Walid Harizi, Zoheir Aboura

ADVANCED MULTIFIELD MODELS FOR WAVES PROPAGATION ANALYSIS IN METALLIC PANELS

Jamal, Najd[a,b], Enrico, Zappino[a], Erasmo, Carrera[a], Walid, Harizi[b], Zoheir, Aboura[b]

a: Mul2 Group, Department of Mechanical and Aerospace Engineering, Politecnico di Torino, Torino, Italy (jamal.najd@polito.it)
b: Université de Technologie de Compiègne, Roberval, Compiègne Cedex, France

Abstract: *Active health monitoring of structures throughout their life cycle is a privilege in the different industrial domains. However, it is essential to the domains where the structures are made of composite materials due to the complex damage mechanisms involved compared to metals* [1] *and due to the absence of an accurate numerical model that permits the prediction of their failure. In this work, the assessment of a multifield layer-wise finite element dynamic plate model (MUL2) based on the Carrera Unified Formulation (CUF) is conducted, on an isotropic aluminum material strip, in order to verify the validity of the model and to finely tune the parameters needed to accurately model wave propagation in the future in laminated material of orthotropic nature. The convergence of the plate model was studied under different modeling parameters, including mesh density, to-the-thickness kinematic model, plate element type and the number of timesteps.*

Keywords: Wave propagation; Lamb waves; Plate model; Carrera Unified Formulation (CUF)

1. Introduction

Composite structures have by nature a complex damage mechanism. This requires the use of different measures to monitor the health of structures made by these materials. The use of various non-destructive testing (NDT) approaches has been studied for the past several decades so that the health of the structure can be determined without affecting its integrity. This is where the application of elastic guided waves propagation in structures excelled for the inspection of structures. Out of these waves, we can mention and focus on Lamb waves that propagate in elastic solid plates with free boundaries. These waves have a displacement direction that is both parallel and perpendicular to the midplane of the plate. Lamb waves have two unique modes of propagation found in isotropic plates, known as symmetric (S) and antisymmetric (A) modes. They are characterized of being the dispersive kind, and the number and nature of modes propagating in a plate depends on the excitation frequency imposed [2]. It can be noticed that for the lower values of frequency-thickness, the excited modes are the fundamental S_0 and A_0 modes exclusively. Among these modes, it is desired to choose the excitation frequency-thickness so that the dispersion effect is relatively low. This can be done by plotting the solution equations of the Lamb wave propagation, named dispersion curves and checking the domain where the velocities are almost constant. As the propagation of these waves is fairly simple in isotropic materials, the taken example under which convergence was studied involves an isotropic aluminum strip. This is also due to the validity of a benchmark with all the properties needed to model wave propagation.

2. Refined Numerical FE Model

The numerical FE model utilized is the MUL2 model, which is based on the Carrera Unified Formulation. In this model, the mechanical 3D displacement vector u (x, y, z) can be split into two terms. The first term, along the xy plane, which has to do with the FEM 2D mesh, and a second term, along the thickness z, that deals with the kinematics of the used model.

$$u(x, y, z) = u_\tau(x, y).F_\tau(z)$$

In commercial FEM programs, it is possible to tune the first terms by deliberately reducing mesh size, increasing the mesh density, or by changing the type of the shell element used. However, it is not possible to tune the second item which deals with the plate kinematics. This means that no matter how much the refined mesh may be, the solutions available can not deliver highly accurate results compared to a 3D model. Using a higher order expansion to-the-thickness allows for the modeling of 3D problems using plate models. This higher order expansion can either be in the form of an equivalent single layer (ESL) referred to as TE, where the whole plate thickness is considered as one layer and Taylor Expansion polynomials are used to the specified order; or it can be a Layer-wise expansion (LW) referred to as LE, where Lagrange Polynomials (linear B2, quadratic B3, or cubic B4) are used in each layer.

In TE for the nth order (TE*n*), the second term $F_\tau(z)$ is written in the terms of z^n where n is the order of the expansion. Taking the third order as an example, the general displacement is given as:

$$U = 1.U_0 + z.U_1 + z^2\,U_2 + z^3\,U_3$$

Where U_i are the unknowns of the problem and U representing the displacement vector {u,v,w}

For LE on the other hand, and taking the linear B2 element as an example, the displacement vector U can be written in terms of linear Lagrange polynomials F_1 and F_2 as:

$$U = F_1U_1 + F_2U_2$$

Where U_1 and U_2 are the actual displacements at the top and the bottom of the plate element, and the polynomials F_1 and F_2 are given by:

$$F_1 = \frac{1+\varsigma}{2} \quad and \quad F_2 = \frac{1-\varsigma}{2}$$

Where -1< ς < 1. On the top, ς =1, F_1 = 1 and F_2 =0. On the bottom, ς =-1, F_1 = 0 and F_2 =1

It can be referred to [3,4] for more information about the Taylor and in refined plate models.

3. Benchmark problem

In this work, the propagation of both fundamental modes was studied using a dynamic numerical analysis which composes of an assessment of the problem regarding the different numerical parameters. In order to efficiently compare the different variations, it is important to specify a guideline to compute the propagation of the ultrasonic waves. The used setup was the one mentioned in [2]. The wave propagation was studied in a thin plate of a 2 mm thickness, a width of 10mm and a length of 500mm. A set of boundary conditions was applied at the boundaries along the width limiting the displacement in the X-axis and ensuring the

unidirectional propagation of the wave along the y direction. A left boundary condition was applied at the plane y=0 as proposed by the benchmark reference mentioned above. The shape of the excitation force imposed is shown in Eq. (1). The two forces are applied perpendicularly and of equal magnitude through time. However, the direction of the forces might differ. Opposite forces produce symmetric waves whereas if both forces have the same direction, antisymmetric waves are generated. In this paper, the applied forces are of opposite direction leading to fundamental symmetric wave generation (S_0). The shape of the load is shown in Eq. (1),

$$F(t) = \tilde{F} sin\omega t \sin^2\left(\frac{\omega t}{2n}\right) \quad (1)$$

where $\omega = 2\pi f$ represents the proper pulsation with the central frequency f and n represents the number of cycles within the signal. The central frequency was chosen so that there would be only a single mode of excitation present, such that $f.d < 1.5\ MHzmm$ according to the dispersion curves in Figure 1 of a 2mm thick aluminum plate of mechanical characteristics found in Table 1.

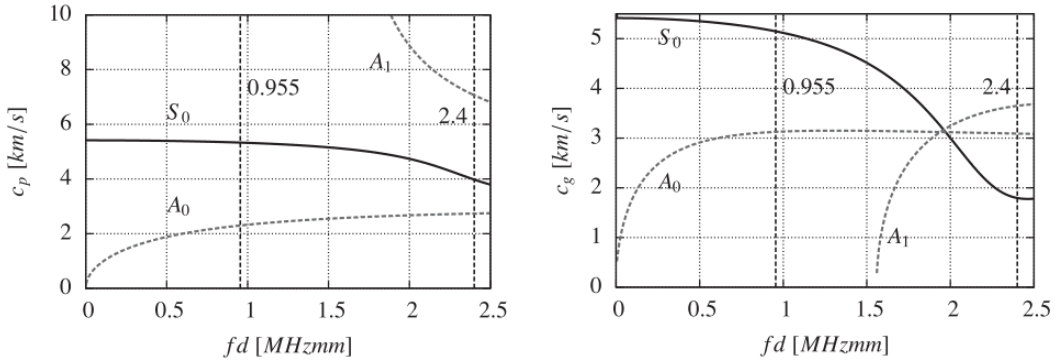

(a) Phase velocities *(b) group velocities*

Figure 1. Dispersion curves of 2mm aluminum plate showing (a) phase and (b) group velocities of the antisymmetric modes (A_i) 'dashed' and the symmetric modes (S_i) 'continuous' [2]

For this reason, the excitation frequency was chosen to be $f = 477.5\ kHz$ with $n = 32$. To study the convergence behavior, two points were chosen (A and B) located on the top of the plate and on the midplane. The position of these points along the y-axis is respectively l_A and l_B(Figure 2)

Table 1 . Material data for aluminium

Youngs modulus (E)	Poisson's ration (ν)	Mass density (ρ)	Longitudinal speed (c_y)	Transversal speed (c_x)
$7 \times 10^{10} \frac{N}{m^2}$	0.33	$2700 \frac{kg}{m^3}$	$6197 \frac{m}{s}$	$3121 \frac{m}{s}$

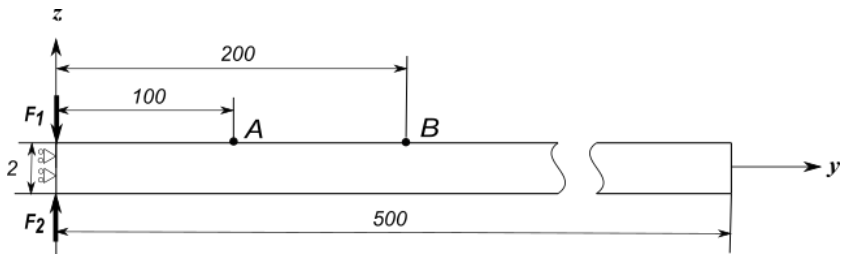

Figure 2. Benchmark of a 2mm aluminum plate showing the distances and the applied forces

4. Evaluation Methodology

The quality of the numerical tool was determined by numerically computing the time-of-flight (TOF) of the propagating Lamb wave packet between points A and B in Figure 3, and comparing this time to an analytical time, computed here by assuming a wave velocity similar to that of the analytical group velocity from the dispersion curves, according to the mode being excited (Table 2). In order to estimate the time at each point, the envelope of the propagating wave had to be generated from the u_z displacement using the Hilbert transform Eq. (2 & 3).

$$H_{A,B}\big(u(t)\big) = \frac{1}{\pi}\int_{-\infty}^{\infty} u_{A.B}(\tau)\ .\ \frac{1}{t-\tau}\ d\tau \tag{2}$$

$$e_{A,B} = \sqrt{H_{A,B}\big(u(t)\big)^2 + u_{A.B}(t)^2} \tag{3}$$

Table 2. Phase and group velocities obtained from dispersion curves [4]

$c_{p_{S0}} \cong 5316\frac{m}{s}$	$c_{p_{A0}} \cong 2298\frac{m}{s}$
$c_{g_{S0}} \cong 5130\frac{m}{s}$	$c_{g_{A0}} \cong 3126\frac{m}{s}$

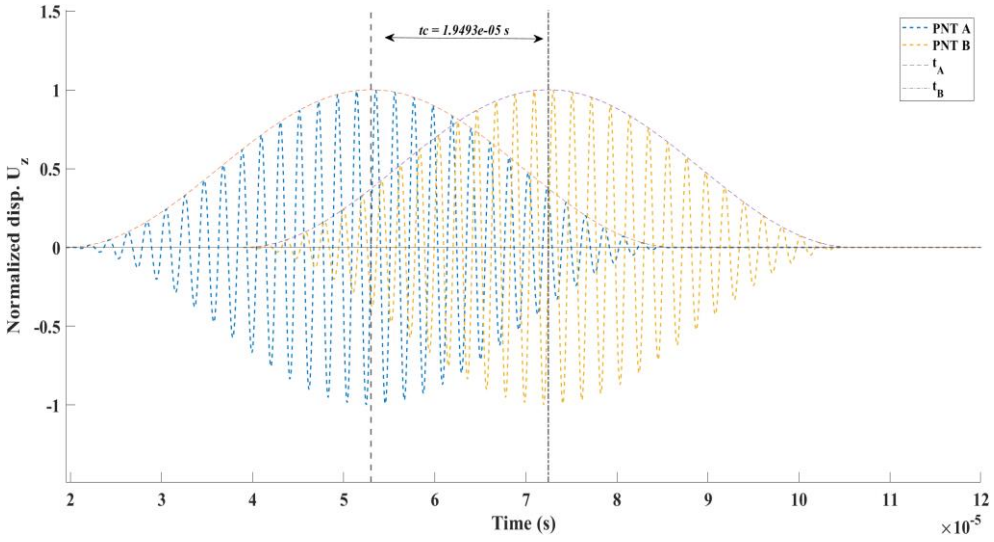

Figure 3. Normalized analytical displacement U_z at points A and B with $t_{c_{ana}}$

The centroid representing the time of each envelope was obtained Eq. (4). This was done using MATLAB commands and coding. The difference of the computed time between point B and A denoted by t_c. Eq. (5) is the time needed for the wave to travel from point A to B.

$$t_{A,B} = \frac{\int_0^{t_{end}} e_{A,B}(t).t\ dt}{\int_0^{t_{end}} e_{A,B}(t)} \tag{4}$$

$$t_c = t_B - t_A \tag{5}$$

And the calculated relative error is the percentage difference between the analytical and the numerical TOF of points A and B, it is calculated as it is seen in Eq. (6)

$$Error\ (\%) = \frac{t_{cana} - t_{cnum}}{t_{cana}} \times 100 \tag{6}$$

5. Assessment Results and Discussion

5.1 Plate element type

The type of the plate elements used was varied between three. The linear element type consisting of 4 nodes, the quadratic type consisting of 9 nodes per element and the cubic type consisting of 16 nodes per element. These elements are denoted by Q4, Q9 and Q16 respectively. Only one element was imposed to the width and the mesh density to the direction of propagation of the wave was altered between 100 to 2000 elements, 4000 for Q4 elements to show convergence. The results in Figure 4 show the convergence of the error with respect to the degrees of freedom according to the number of elements used in each of the three plate element types. Note that this was done for a fixed to-the-thickness Taylor expansion of the third order TE3 and with 2000 timesteps between 0 and 120 µs. It can be clearly shown that the higher order elements (Q9 and Q16) converge faster, for a lower mesh density, than the lower order. But these elements already have higher DOF for each element. The low mesh density leads to a stiff structure which explains the high error at the beginning of the curves.

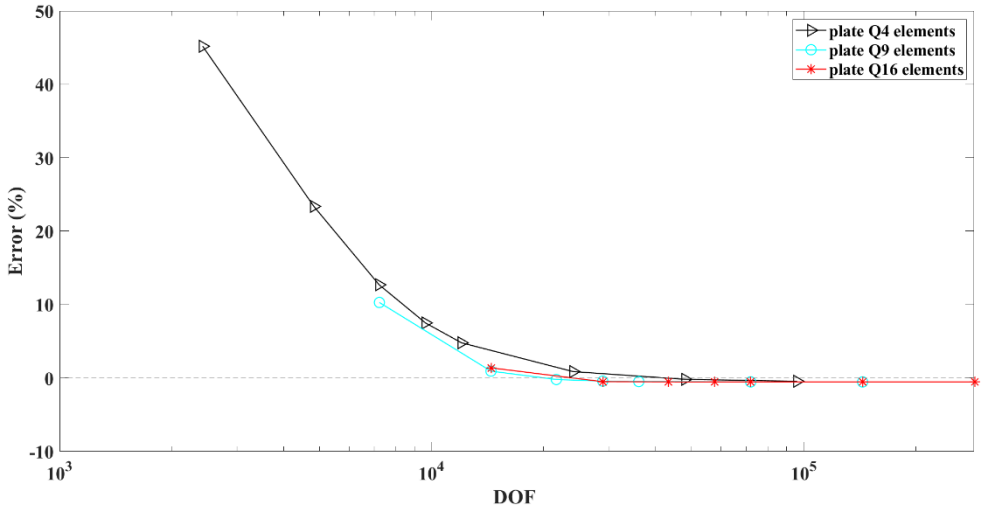

Figure 4. Convergence of different plate element types according to the degrees of freedom

5.2 Model kinematics

The convergence of the problem with different model Kinematics, or to-the-thickness expansion, was also studied in this paper. The Kinematics range between Taylor 1 to 4th expansion, and Lagrange expansion of linear, quadratic and cubic elements denoted by B2, B3 and B4 respectively, where 2B4 means two cubic elements of expansion. These models were compared with one another under the same plate element type, using the same timestep mentioned above (2000 timesteps between 0 and 120 µs) but under different mesh density to the thickness. The classical plate theories such as classical lamination theory and first order shear deformation theories fail to capture wave propagation through the structure. The results shown in Figure 5 show clearly the convergence of the out of plane expansions to different values. Noting that the linear expansion of both Taylor and the one Lagrange element to-the thickness have exactly the same results with the same DOF. The same goes for TE2 and LE B3, and to TE3 and LE B4. The advantage of using Lagrange expansion lies in the ability to impose boundary conditions on the top and bottom nodes of the plate separately. Also using many elements to the thickness for layered structures, i.e. composites, to accurately depict their behavior.

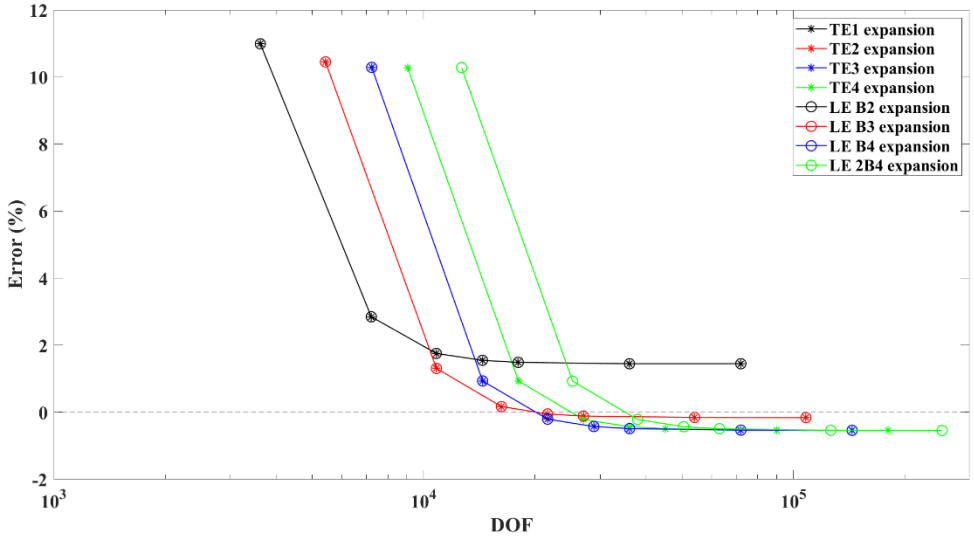

Figure 5. Convergence analysis of the different out of plane expansions according to the degrees of freedom

It is also clearly shown in Figure 6, where the results were plotted with respect to the mesh number along the thickness. It is true that the convergence value of the higher order expansion has a higher error in these results, but this is mainly due to the choice of the timestep as the next results will bring to light.

5.3 Time step analysis

As mentioned above, the effect of the timestep number within the modeling time ranging from 0 to 120 µs was studied for only one case. The chosen case was a structure having Q9 elements and with TE3 (or LE B4) expansion as these produce the same results for a one layered structure. The reason behind choosing this order of expansion lies in the fact that the higher order expansions used in the comparison (TE4 and LE 2B4) converged to the same values as that of this expansion but for a higher computational cost, see Figure 5. The number of timesteps chosen was 500, 1000, 2000 and 4000. The analysis was done for different mesh densities as earlier.

The results of Figure 7 show the clear relation between minimizing the time step (using more steps) to the convergence towards the analytical value. The lower the timestep is, the more accurate the value of convergence, for the same model kinematics. This is due to the higher accuracy of the imposed variable load at lower timesteps and due to the higher accuracy during the integration of the produced displacement curve under higher value of timesteps.

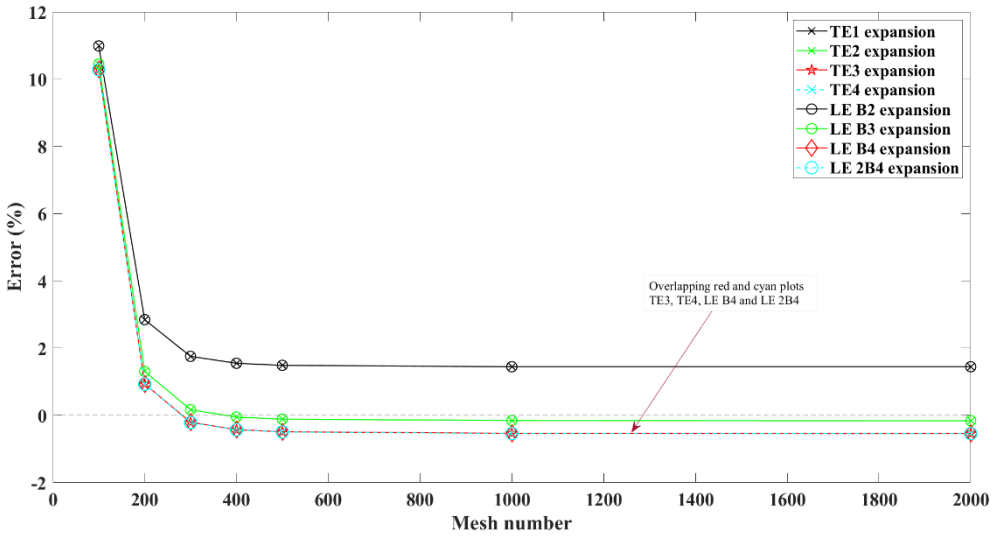

Figure 6. Convergence analysis of the different out of plane expansions w.r.t mesh number

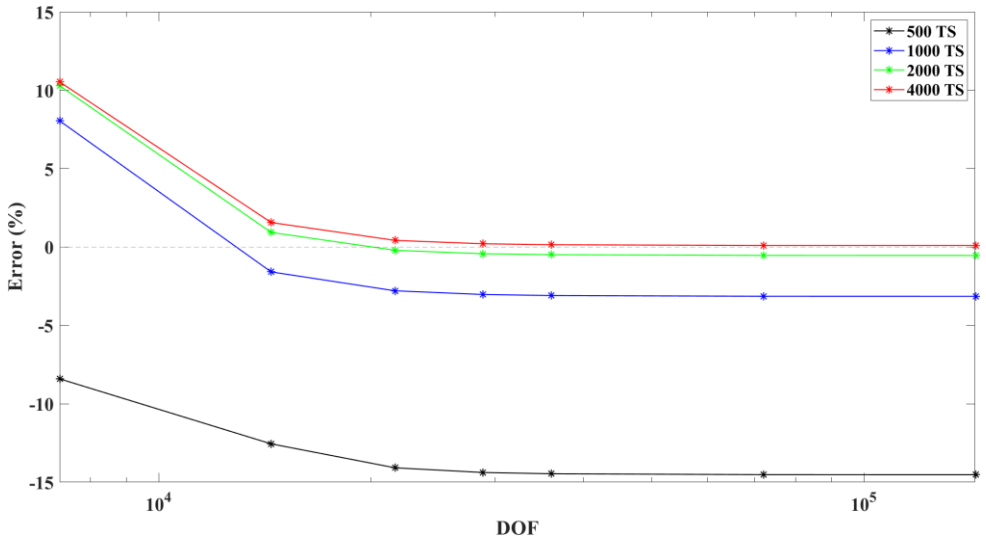

Figure 7. The effect of the number of timesteps (timestep estimate) on the convergence value

6. Conclusion

The numerical assessment of symmetric Lamb wave propagation using a Variable Kinematics model was studied for isotropic aluminum material on the premise of validating the model for further use in laminated and smart structures. The findings of this work show that this model can accurately predict the propagation of the symmetric Lamb waves in isotropic material. If

plate models were to be used, the most suitable element types would be either Q9 or Q16 elements, as Q4 elements are highly not recommended due to the low accuracy. The number of elements used differ according to the element type used, as Q16 elements can reach the same accuracy of Q9 elements for a lower number of elements but on the expense of DOF compared to that of Q9. As for the plate kinematics, or to-the-thickness expansion, the cubic to-the-thickness expansion (TE3 or LE B4) was enough. To reach a higher accuracy in modeling and convergence, a more refined timestep should be used, leading to the use of almost 4000 timesteps in the time domain of the model. To check the validity of the in general expressions mentioned in [4], with a timestep $\Delta t < \frac{1}{20\, f_{max}}$ and mesh size $L_{min} < \frac{\lambda}{10}$, and where $\lambda = \frac{c_y}{f}$. In order to get an error of less than 1%, according to our results it is better to choose a timestep $\Delta t < \frac{1}{30 f_{max}}$ with a cubic expansion to-the-thickness, as $\Delta t < \frac{1}{20\, f_{max}}$ gives a round 1200 timesteps, leading to a higher convergence error. The minimum mesh size is chosen to be $L_{min} < \frac{\lambda}{8}$ when using Q9 plate elements and $L_{min} < \frac{\lambda}{5}$ when using Q16 plate elements, thus a general mesh size of $L_{min} < \frac{\lambda}{10}$ as proposed in the reference before is acceptable.

Acknowledgements

The authors would like to thank the Hauts-de-France Region (France) and Politecnico di Torino (Italy) for the funding of this work as part of the doctoral thesis of Mr. Jamal NAJD (Agreement number 20003877, N◦ GALIS: ALRC2.0-000072).

1. References

1. Jollivet T, Peyrac C, Lefebvre F. Damage of composite materials. In: Procedia Engineering. Elsevier Ltd; 2013. p. 746–58.

2. Giurgiutiu V. Structural health monitoring with piezoelectric wafer active sensors. 16th International Conference on Adaptive Structures and Technologies. 2006. 94–100 p.

3. Carrera E, Cinefra M, Zappino E, Petrolo M. Two-Dimensional Shell Models with Nth-Order Displacement Field, the TE Class. In: Finite Element Analysis of Structures Through Unified Formulation [Internet]. John Wiley & Sons, Ltd; 2014. p. 231–51. Available from: https://onlinelibrary.wiley.com/doi/abs/10.1002/9781118536643.ch11

4. Carrera E, Cinefra M, Zappino E, Petrolo M. Two-Dimensional Models with Physical Volume/Surface-Based Geometry and Pure Displacement Variables, the LE Class. In: Finite Element Analysis of Structures Through Unified Formulation [Internet]. John Wiley & Sons, Ltd; 2014. p. 253–60. Available from: https://onlinelibrary.wiley.com/doi/abs/10.1002/9781118536643.ch12

5. Willberg C, Duczek S, Vivar Perez JM, Schmicker D, Gabbert U. Comparison of different higher order finite element schemes for the simulation of Lamb waves. Comput Methods Appl Mech Eng [Internet]. 2012;241–244:246–61. Available from: http://dx.doi.org/10.1016/j.cma.2012.06.011

6. GARCIA DE MIGUEL A. Hierarchical component-wise models for enhanced stress analysis and health monitoring of composites structucres. Politecnico di Torino; 2019.

7. Alem B, Abedian A, Nasrollahi-Nasab K. Reference-Free Damage Identification in Plate-

Like Structures Using Lamb-Wave Propagation with Embedded Piezoelectric Sensors. J Aerosp Eng. 2016;29(6):04016062.

